On the estimate of near fields for the WEST ICRF travelling wave array launcher

Riccardo Ragona[1*], *Vincent* Maquet[2], and *Julien* Hillairet[3]

[1]Department of Physics, Technical University of Denmark, Lyngby, Denmark
[2]Laboratory for Plasma Physics, Royal Military Academy, Bruxelles, Belgium
[3]CEA, IRFM, F-13108 Saint-Paul-lez-Durance, France

Abstract. This study focuses on the Ion Cyclotron Range of frequency (ICRF) Travelling Wave Array (TWA) launcher proposed for the WEST tokamak. This launcher aims to mitigate the detrimental effects associated with resonant ICRF launchers, currently used in most magnetic plasma confinement experiments. The WEST TWA launcher, characterized by reduced near fields and an optimized spatial spectrum, is compared to current WEST ICRF launchers. The parallel component of the electric field on the limiters is particularly investigated, which is a proxy for sheath rectification and impurity production. Full-wave modelling using ANSYS HFSS software, paired with an in-house Python library, was employed to simulate the near fields generated by the TWA and WEST ICRF launchers. The models use experimental equilibrium and plasma profiles from a WEST discharge, with perfect electric conductor boundaries and artificial loss added to the plasma dielectric tensor to damp wavefield amplitude away from the launcher. Results indicate that the TWA launcher present design significantly reduces the amplitude of the toroidal components of the electric field on the limiter surfaces by a factor of more than four compared to the WEST ICRF launchers, which is expected to reduce the impurity production.

1 Introduction

Ion cyclotron resonant heating (ICRH), an ICRF technique used to deposit energy to the ions in magnetized plasmas, can provide several functionalities like core ion heating, sawteeth control, plasma start-up and landing, and wall cleaning. A key component of an ICRH system is the launcher, which transfers the generator power to the plasma. The waves in the ion cyclotron range of frequencies are evanescent in the thin scrape off layer plasma and become propagative only once they reach a certain density. The launcher needs to provide a high field to bridge this gap, which in the region of the launcher, could give rise to detrimental effects. A large electric field parallel to the background magnetic field is expected to produce sputtering of impurities from the metal surfaces magnetically connected with the launcher, which diffusing into the main plasma, remove energy.

Several mitigation techniques have been envisaged to reduce the detrimental effect of large electric fields. For example, the electromagnetic field spectrum coupled at the aperture could be optimized to reduce the interactions with the wall [1]. Traditional launchers, like the one installed on WEST [2], use Faraday screens to reduce the parallel component of the field. In contrast, a Travelling Wave Array (TWA) launcher shows reduced near fields [3] and its coupling spectrum could be optimized to reduce the content of unwanted modes.

The TWA system proposed for WEST [4,5] consists of two launchers, as shown in Figure 1 with an overview of the WEST internal systems. The TWA is in sector Q4, near the ECRH launcher located in sector Q3. There are two rows of radiating elements displaced poloidally above and below the equatorial plane. A single vessel port is used to support and feed the antenna with cooling and RF power. Two lateral limiters define the radial position of the antenna.

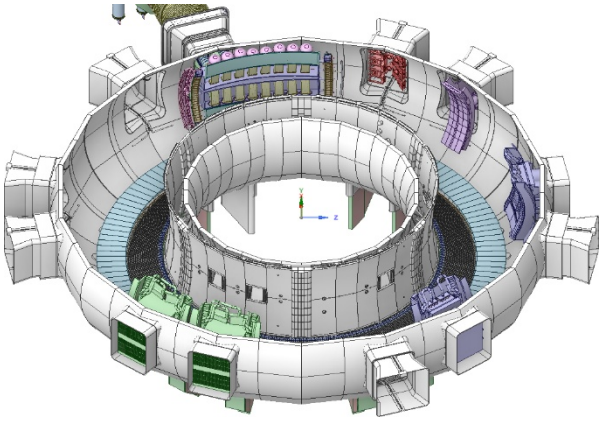

Fig. 1. Overview of the WEST internal systems with the two TWA launchers in the centre-top of the figure. The other components are (in clockwise direction): the ECRH launcher, the main movable limiter, the two ICRF launchers, and the two LH launchers.

In this contribution we report on the preliminary analysis of the near field generated by the TWA launchers. As discussed in section 2, we focus on the parallel component of the electric field on the limiters, as it is recognized as a proxy for the sheath rectification, thus related to impurity production. The models and methods are presented in section 3. In section 4 we show how this component of the field differs between the TWA and the WEST ICRF launchers, when calculated for the same plasmas.

* Corresponding author: ricrag@fysik.dtu.dk

2 RF sheath - near fields - impurities

An RF sheath [6] is a dynamic, non-neutral plasma region that forms near surfaces exposed to RF electromagnetic fields, such as the metallic walls in fusion devices. An RF sheath is driven by oscillating electric fields, leading to time-varying charge separation and non-linear effects.

When RF waves interact with a plasma boundary, electrons respond rapidly to the RF fields, while slower ions lag, creating a periodically expanding and collapsing sheath layer. This process generates a rectified DC potential, accelerating ions toward the surface and contributing to material erosion and impurity generation, which are critical concerns for fusion reactors.

In fusion devices, these sheaths form near ICRF antennas and other RF components, modifying the edge plasma behaviour and affecting the overall device performance [7]. Mitigation strategies, such as optimizing launcher design, aligning it to magnetic fields, and using gas injection, aim to minimize detrimental sheath effects while maintaining effective plasma heating [8].

Two successful examples of such mitigations are the 3-strap antenna system in ASDEX Upgrade [9] and the field-aligned antenna in Alcator C-MOD [10]. The first reduces the impurity produced during the launcher operation by minimizing the excitation of the current density parallel (to the background magnetic field) component on the launcher frame. It achieves that by using three straps where the centre one is in anti-phase and carries twice the current of the side straps. The second strategy aligned the launcher with the background magnetic field to reduce the local parallel component of the electric field.

Seeking for the minimization of the parallel component of the electric field is justified by the correlation between RF sheaths and $E_{//}$. Reducing the amplitude of $E_{//}$ will reduce the RF sheath (rectified) potential, which is the driver of impurity production via sputtering by ions accelerated by the sheath potential itself [11]. The amplitude of $E_{//}$ could then be used as proxy for the sheath potential. The reduction of ICRF-driven impurity release is of paramount importance for the applicability of any ICRF tool in future reactors.

3 Models and methods

The analysis presented here is based on full-wave modelling carried out with the ANSYS HFSS [12] commercial software paired to an in-house python library [13]. This library allows building the parametric model, creating the suitable plasma material, running the simulations, and manipulating the result data. The plasma material used in HFSS is created based on the experimental equilibrium and profiles of WEST discharge #56898 (I_p=500 kA, n_l=4x10^{19} m^{-2}, P_{IC}=2.5 MW). This data is used to create datasets representing the tensor components, in cylindrical coordinate, inserted in the HFSS material definition. Figure 2 shows the poloidal flux contours together with the last closed flux surface (LCFS). The electron density

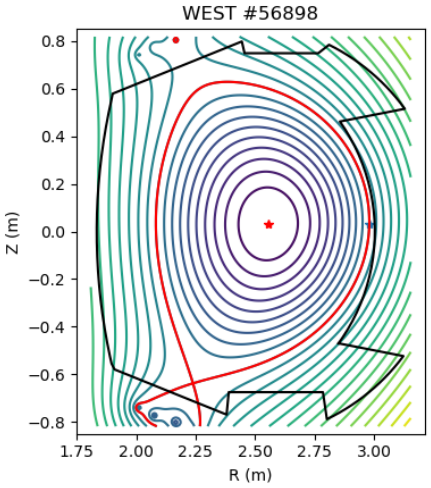

Fig. 2. Poloidal flux contours for the equilibrium of WEST discharge #56898 used as reference for the calculations. The red line represents the last closed surface.

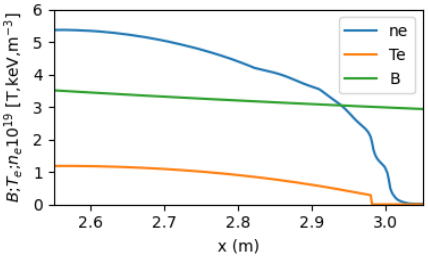

Fig. 3. Radial profiles of the electron density and temperature, and of the magnetic field for the reference discharge #56898.

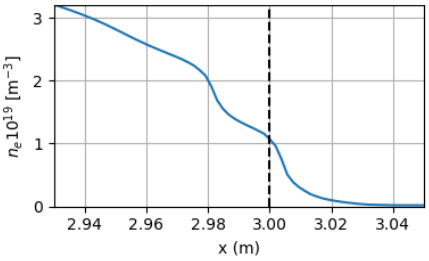

Fig. 4. Detail view of the density profile of Figure 3 in the region of the LCFS (2.98 m). The antenna limiter location is marked with the dashed line.

and temperature profiles are shown in Figure 3 along with the toroidal magnetic field. Figure 4 is a detailed view of the edge density profile with the LCFS located 2.98 m and the antenna limiters at 3.0 m.

Two HFSS models were built for this investigation: one of the WEST ICRF launchers, and the other of the TWA launcher. The first model is shown in Figure 5. Only a part of the WEST vessel volume around the launcher is considered in the simulation. Perfect electric conductor (PEC) is applied as boundary condition (BC) on the simulation domain. An artificial loss is added to the plasma dielectric tensor to damp the wavefield amplitude and reduce/avoid reflections at the boundaries, far from the antenna aperture. This model has four input ports, each assigned to a waveport excitation. An equivalent model for the TWA launcher is created, using the same BCs and plasma material. This

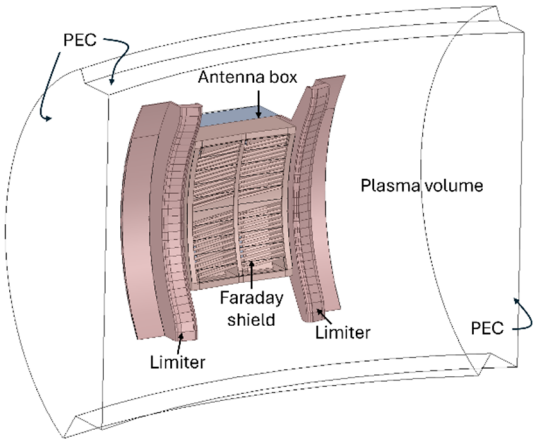

Fig. 5. HFSS model of the WEST ICRF launcher with the main components and boundary conditions labelled.

model has 20 ports, each assigned to a waveport excitation. Four of those ports are for input/output and the remaining 16 are for the capacitors. In both cases, the internal volume of the launchers' boxes and of the feeding transmission lines is modelled as vacuum.

The simulation solutions are used to compute the fields on the surfaces of interest. In our case, those surfaces are the limiters surfaces. The excitations used to calculate the fields are as follows.

For the WEST ICRF launcher, the solution S-matrix is used as input for the WEST_IC_antenna code, a Python numerical model of the ICRH antenna system. The code calculates the matching solution for the two launcher halves and provides the input voltages to apply to the HFSS model corresponding to the requested coupled power.

For the TWA, the HFSS 20-port S-matrix solution is coupled to the circuit solver (ANSYS) Designer. With the proper capacitor layout connected, and the requested input power, the excitations are pushed-back to HFSS for calculating the fields. At this stage is possible to evaluate the single transit coupling (STC) of the rows and to adjust the input power on the feeding ports to obtain the desired coupled power.

The quantity of interest is the parallel component of the electric field, $E_{//}$, evaluated on the limiter surfaces. However, to simplify the calculation, the quantity used is instead the toroidal component of the electric field, E_{tor}. This is in good approximation equivalent to $E_{//}$ due to the small pitch angle of the WEST magnetic field lines at the antenna location (~4 to 5 degrees). The generated error is considered negligible.

4 Results

The comparison between the WEST ICRF launcher and the TWA is made by imposing the same amount of coupled power from the two systems. This value is chosen to be 2 MW. For the WEST ICRF launcher, this is equivalent to a 1 MW of coupled power for each side of the launcher, which is the power delivered by the generators (one per side). For the TWA launcher to couple 2 MW in the coupling conditions of the selected discharge (~80% STC), each row requires an input power of ~1.25 MW.

The amplitude of the toroidal components of the electric field is calculated on the limiters surfaces and is shown in Figure 6. The top part of the figure shows the WEST ICRF launcher seen from the front, while the bottom part shows the TWA launcher. The colour scale is linear. The TWA launcher has been cut to ease the comparison, showing only the first and last straps of each row and aligning the view look at the limiter from the front. The dashed line represents the mid axis of the launchers. The TWA is fed from the left side, and both rows are fed. The difference is remarkable. The TWA shows a reduction of the fields of a factor greater than four.

The TWA launcher is composed of two independent rows, and the isolation between them is better than 25 dB. These two launchers are both powered by an independent generator. An arbitrary phase difference could be imposed on the generators, and consequently on the launchers. The amplitude of the electric field toroidal component on the limiters' surfaces for four different values of the phase difference between generators is shown in Figure 7 for the left (seen from

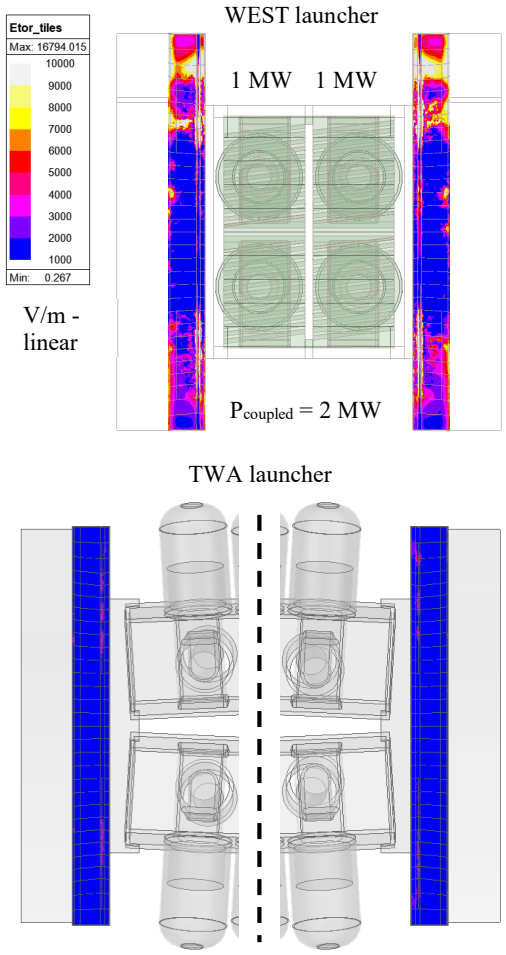

Fig. 6. Toroidal component of the electric field on the limiter surfaces (top) of the WEST ICRF launcher, and (bottom) of the TWA launcher. The coupled power is set to be 2 MW for both systems. The colour scale is linear. The TWA shows a considerable reduction in amplitude.

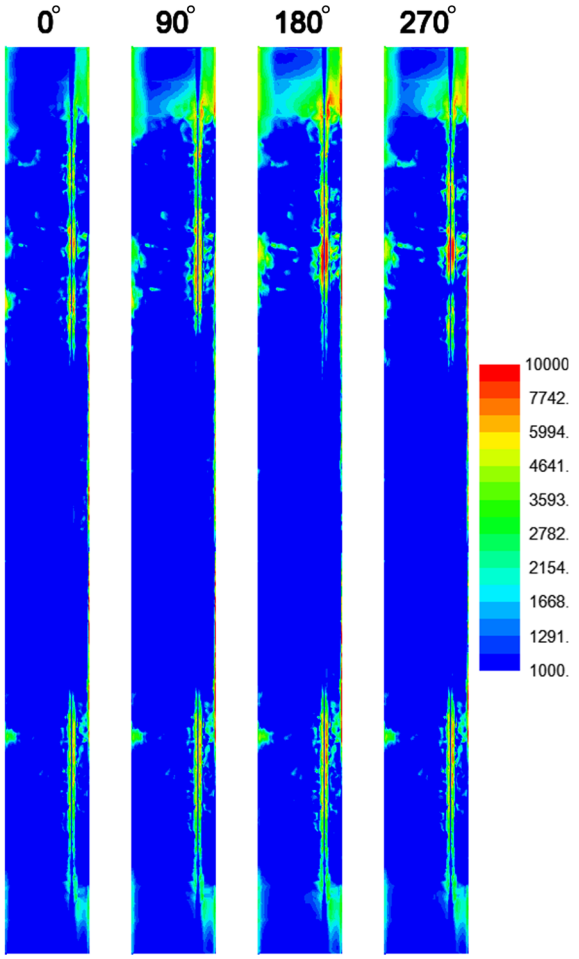

Fig. 6. Toroidal component of the electric field on the left-limiter surfaces. Four phase difference values between the rows are depicted showing the impact of phasing on the distribution and intensity of the field amplitude. The difference is mainly in the amplitude with only minor changes in its distribution on the surface.

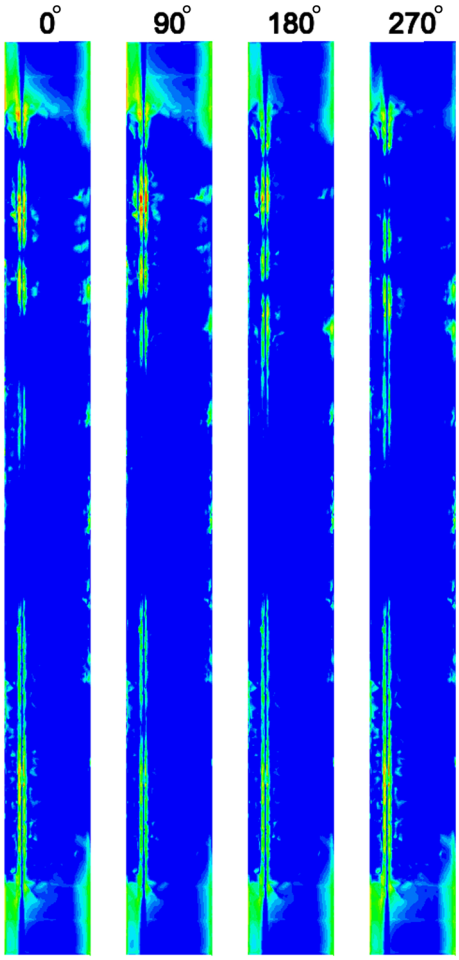

Fig. 5. Same as Figure 7 but for the right limiter. Here the difference is more on the distribution of the field rather than on the amplitude, especially on the upper half.

the plasma) limiter, and in Figure 8 for the right limiter. The field amplitude could be expected to be greater on the left side than on the right side, as the left side is the fed one, and due to the presence of a good antenna loading (80% STC). In fact, an overall increase in amplitude is observed on the left limiter. However, there are some notable differences in the field amplitude distribution for the different phasing. The upper half of both limiters has the largest variation presenting different patterns for the maxima location. The bottom halves display minor changes.

5 Discussion

The TWA launcher offers a promising reduction of E_{tor} when compared to the WEST ICRF launcher, for the same amount of coupled power. The small pitch angle of the magnetic field at the launcher's location ensures a small error when considering E_{tor} instead of $E_{//}$ as figure of merit. However, the same approximate Figure of merit is used for both models allowing for a consistent comparison. The results presented here suggest that the TWA launcher can reduce the sheath potential, thus reducing the impurity production from the limiters. Additional more elaborate analysis is needed to consolidate this result.

In the design of the TWA launcher, mitigation strategies as described in [14] were incorporated since the beginning. The radiating elements are further away from the launcher´s box, as seen in fig. 6. Additionally, the power density is reduced due to the larger aperture surface.

One may argue that the reduction in near fields is only due to the larger number of toroidal radiating elements which reduces the power density and the poloidal field per element. However, the antenna apertures ratio is ~3 and the reduction in voltages (average value) is ~2-3, which does not correspond to the observed value. We consider this reduction to be a combination of the above-mentioned strategies which have a clear correlation with the minimization of the low $k_{//}$ components of the launcher power spectrum [1]. For reference, an example of optimized TWA spectrum together with its sensitivity to operational parameters is given in [3].

Traditionally, ICRF launchers are equipped with a Faraday Shield (FS) on the apertures, like the one on the WEST ICRF launcher (see fig. 5 and 6-top). This structure has the main function of protecting the strap from the plasma. Additionally, the conductor bars could

behave like a polarizer, reducing the field component parallel to them. The WEST TWA launcher, however, does not have a FS. Preliminary analysis showed that adding a FS does not reduce the fields considerably, and a more detailed analysis on the impact of the FS on both type of launchers will be presented in a subsequent publication.

The results presented here shows that the field amplitude pattern on the limiters depends on the phase between the two launcher's rows. The possibility of arbitrarily controlling this phase could allow finding an optimal configuration which reduces the near fields on the limiter surfaces. The figure of merit to carry out this optimization is under discussion. However, this optimization should also consider the effect of the phasing on the absorption, as described in [15,16]. A future work will identify if an optimal phase that reduces E_{tor} exists.

One aspect missing in this preliminary analysis is the effect of different plasma loading on the launchers near fields. Besides requiring a greater input power to obtain the same value of coupled power, lowering the plasma loading on the TWA, i.e., increasing distance from the LCFS, results in larger and more homogeneously distributed fields on the launcher structure. However, this increase in fields amplitude is expected to be lower than the increase in field for the WEST ICRF launcher, with the TWA maintaining its improved performance with low associated impurity production.

This work has been carried out within the framework of the EUROfusion Consortium, funded by the European Union via the Euratom Research and Training Programme (Grant Agreement No 101052200 — EUROfusion). Views and opinions expressed are however those of the author(s) only and do not necessarily reflect those of the European Union or the European Commission. Neither the European Union nor the European Commission can be held responsible for them.

References

[1] V. Maquet and A. Messiaen, Optimized phasing conditions to avoid edge mode excitation by ICRH antennas, Journal of Plasma Physics **86**, 855860601 (2020). https://doi.org/10.1017/S0022377820001415

[2] J. Hillairet et al., WEST actively cooled load resilient ion cyclotron resonance heating system results, Nucl. Fusion **61**, 096030 (2021). https://doi.org/10.1088/1741-4326/ac1759

[3] R. Ragona, V. Maquet and J. Hillairet, Status of the radiofrequency modelling of the WEST Ion Cyclotron Travelling Wave Array launcher, Fusion Engineering and Design **218**, 115168 (2025). https://doi.org/10.1016/j.fusengdes.2025.115168

[4] J. Hillairet et al., Design and development of the actively cooled ion cyclotron travelling wave array system for WEST, 25th Topical Conference on Radio-Frequency Power in Plasmas, Schloss Hohenkammer, Germany, May 19-22 (2025). https://www.ipp.mpg.de/5533880

[5] R. Ragona, A. Messiaen, J. M. Bernard, E. Delchambre, R. Dumont, F. Durodié, J. Hillairet, J. Ongena, D. Van Eester, and M. Van Schoor, Traveling wave array for DEMO with proof of principle on WEST, Fusion Engineering and Design **146**, 854 (2019). https://doi.org/10.1016/j.fusengdes.2019.01.097

[6] J. R. Myra, A tutorial on radio frequency sheath physics for magnetically confined fusion devices, Journal of Plasma Physics **87**, 905870504 (2021). https://doi.org/10.1017/S0022377821000878

[7] L. Colas et al., The geometry of the ICRF-induced wave–SOL interaction. A multi-machine experimental review in view of the ITER operation, Nucl. Fusion **62**, 016014 (2021). https://doi.org/10.1088/1741-4326/ac35f9

[8] V. Bobkov et al., Impact of ICRF on the scrape-off layer and on plasma wall interactions: From present experiments to fusion reactor, Nuclear Materials and Energy **18**, 131 (2019). https://doi.org/10.1016/j.nme.2018.11.017

[9] V. Bobkov et al., Making ICRF power compatible with a high-Z wall in ASDEX Upgrade, Plasma Phys. Control. Fusion **59**, 014022 (2016). https://doi.org/10.1088/0741-3335/59/1/014022

[10] S. J. Wukitch et al., Characterization and performance of a field aligned ion cyclotron range of frequency antenna in Alcator C-Mod, Physics of Plasmas **20**, 056117 (2013). https://doi.org/10.1063/1.4803882

[11] Vl. V. Bobkov et al., Assessment of compatibility of ICRF antenna operation with full W wall in ASDEX Upgrade, Nucl. Fusion **50**, 035004 (2010). https://doi.org/10.1088/0029-5515/50/3/035004

[12] ANSYS HFSS, www.ansys.com/products/electronics/ansys-hfss

[13] V. Maquet, R. Ragona, D. V. Eester, J. Hillairet, and F. Durodie, ANSYS HFSS as a New Numerical Tool to Study Wave Propagation inside Anisotropic Magnetized Plasmas in the Ion Cylotron Range of Frequencies, arXiv:2309.14015 (2023). https://doi.org/10.48550/arXiv.2309.14015

[14] V. Bobkov et al., ICRF operation with improved antennas in ASDEX Upgrade with W wall, Nucl. Fusion **53**, 093018 (2013). https://doi.org/10.1088/0029-5515/53/9/093018

[15] P. Vallejos, T. Johnson, R. Ragona, T. Hellsten, and L. Frassinetti, Effect of poloidal phasing on ion cyclotron resonance heating power absorption, Nucl. Fusion **59**, 076022 (2019). https://doi.org/10.1088/1741-4326/ab1ab7

[16] L. Hijazi, J. Hillairet, R. Dumont, V. Maquet, and R. Ragona, Parametric analysis of the TWA launcher for WEST using minority heating ICRH technique, Nucl. Fusion **65**, 106011 (2025). https://doi.org/10.1088/1741-4326/ae004f